N-Glycosylation regulates endothelial lipase-mediated phospholipid hydrolysis in apoE- and apoA-I-containing high density lipoproteins

Danielle Skropeta,[1,*] Chatri Settasatian,[2,*] Monica R. McMahon,[*] Kate Shearston,[*] Daniela Caiazza,[*] Kristine C. McGrath,[*] Weijun Jin,[†] Daniel J. Rader,[†] Philip J. Barter,[*,§] and Kerry-Anne Rye[3,*,§,]**

Lipid Research Group,* Heart Research Institute, Camperdown, New South Wales 2050, Australia; Department of Medicine,† University of Pennsylvania School of Medicine, Philadelphia, PA 19104; Department of Medicine,§ University of Sydney, New South Wales 2006, Australia; and Department of Medicine,** University of Melbourne, Victoria 3010, Australia

Abstract Endothelial lipase (EL) is a member of the triglyceride lipase gene family with high phospholipase and low triacylglycerol lipase activities and a distinct preference for hydrolyzing phospholipids in HDL. EL has five potential *N*-glycosylation sites, four of which are glycosylated. The aim of this study was to determine how glycosylation affects the phospholipase activity of EL in physiologically relevant substrates. Site-directed mutants of EL were generated by replacing asparagine (N) 62, 118, 375, and 473 with alanine (A). These glycan-deficient mutants were used to investigate the kinetics of phospholipid hydrolysis in fully characterized preparations of spherical reconstituted high density lipoprotein (rHDL) containing apolipoprotein E2 (apoE2) [(E2)rHDL], apoE3 [(E3)rHDL], apoE4 [(E4)rHDL], or apoA-I [(A-I)rHDL] as the sole apolipoprotein. Wild-type EL hydrolyzed the phospholipids in (A-I)rHDL, (E2)rHDL, (E3)rHDL, and (E4)rHDL to similar extents. The phospholipase activities of EL N118A, EL N375A, and EL N473A were significantly diminished relative to that of wild-type EL, with the greatest reduction being apparent for (E3)rHDL. The phospholipase activity of EL N62A was increased up to 6-fold relative to that of wild-type EL, with the greatest enhancement of activity being observed for (E2)rHDL. These data show that individual *N*-linked glycans have unique and important effects on the phospholipase activity and substrate specificity of EL.—Skropeta, D., C. Settasatian, M. R. McMahon, K. Shearston, D. Caiazza, K. C. McGrath, W. Jin, D. J. Rader, P. J. Barter, and K-A. Rye. ***N*-**Glycosylation regulates endothelial lipase-mediated phospholipid hydrolysis in apoE- and apoA-I-containing high density lipoproteins.** ***J. Lipid Res.*** **2007.** 48: **2047–2057.**

Supplementary key words *N*-linked glycans • site-directed mutagenesis • apolipoprotein E • apolipoprotein A-I • phospholipase kinetics • Michaelis-Menten constant • maximum velocity • binding affinity

Endothelial lipase (EL) is a recently identified member of the triglyceride lipase gene family (1, 2) that plays a central role in HDL metabolism (1, 3–5). Compared with other members of the gene family, such as LPL and HL, EL has a distinct preference for hydrolyzing phospholipids in HDL and the distinguishing features of high phospholipase and low triglyceride lipase activities (6). The primary amino acid sequence of human EL shows 45% homology with human LPL (7, 8) and 40% with human HL (9). Human EL also shows 27% homology with human pancreatic lipase, the only member of the triglyceride lipase gene family that has been fully characterized by X-ray crystallography (10, 11). Human EL has five potential *N*-glycosylation sites at asparagines 62, 118, 375, 451, and 473. The asparagine residues at positions 62 and 375 are conserved in both murine and rat EL as well as in human, mouse, and rat HL and LPL (12, 13) (**Fig. 1A**). [The five potential glycosylation sites of EL, predicted by the presence of the consensus sequence Asn-Xxx-Ser/Thr, occur at asparagine residues at positions 80, 136, 393, 469, and 491 (1). Miller et al. (12) previously described these positions as 60, 116, 373, 449, and 471; however, they are described here as positions 62, 118, 375, 451, and 473 in the conventional manner, by discounting the 18 residue hydrophobic sequence of the secretory signal peptide (1).]

Overexpression of EL in mice markedly decreases HDL cholesterol and apolipoprotein A-I (apoA-I) levels (1, 3), whereas inhibition of EL in mice increases HDL choles-

Manuscript received 9 May 2007 and in revised form 30 May 2007.

Published, JLR Papers in Press, June 3, 2007.
DOI 10.1194/jlr.M700248-JLR200

Abbreviations: apoE, apolipoprotein E; CE, cholesteryl ester; EL, endothelial lipase; rHDL, reconstituted high density lipoprotein; UC, unesterified cholesterol.

[1] Present address of D. Skropeta: Department of Chemistry, University of Wollongong, New South Wales 2522, Australia.

[2] Present address of C. Settasatian: Department of Pathology, Khon Kaen University, Khon Kaen, 40002, Thailand.

[3] To whom correspondence should be addressed.
e-mail: ryek@hri.org.au

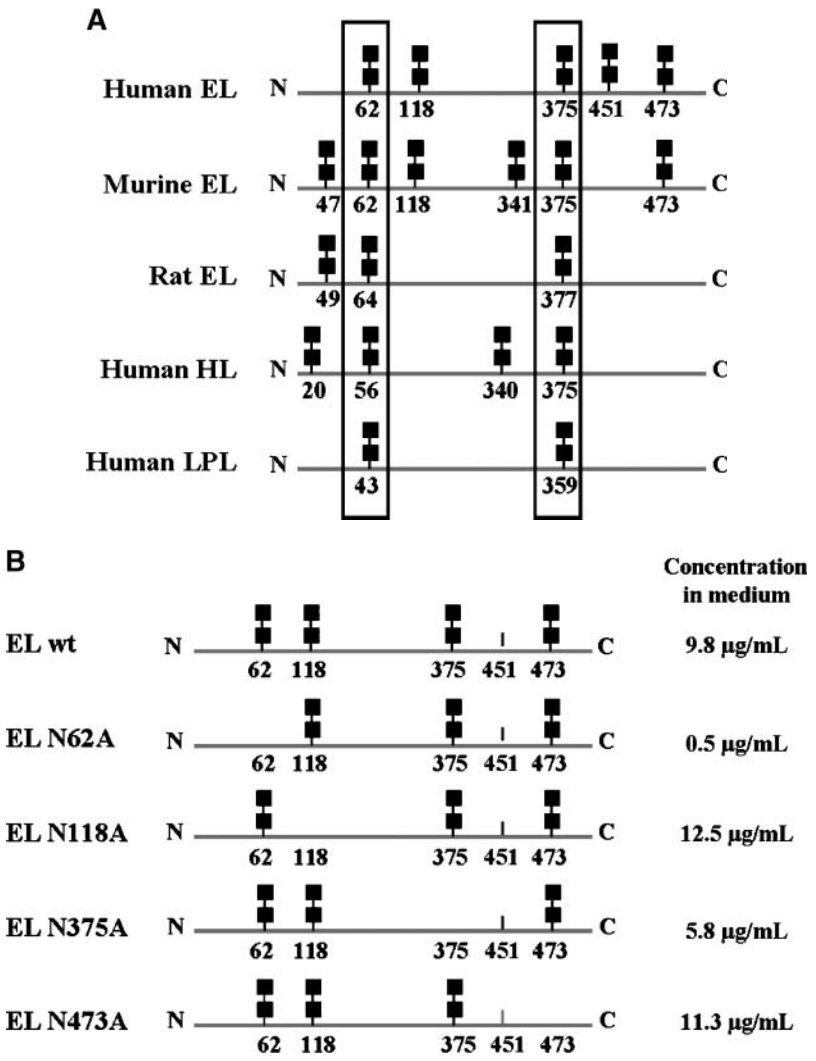

Fig. 1. A: Schematic representation of all predicted *N*-linked glycosylation sites in human endothelial lipase (EL), murine EL, rat EL, human HL, and human LPL. The conserved residues are enclosed in boxes. B: Schematic representation of the *N*-linked glycosylation sites used in wild-type human EL and the site-directed human EL mutants in which individual asparagine residues were replaced by alanine. Nonused sites are represented by dashes, and used sites are represented by short chains. The concentration of wild-type and mutant EL secreted into the medium was determined by ELISA.

terol levels and generates large, potentially antiatherogenic HDL (14). Inactivation of EL in mice by gene targeting also increases plasma HDL cholesterol, apoA-I, and apoE levels and increases HDL size (4). Furthermore, EL is upregulated by inflammatory stimuli such as tumor necrosis factor-α and interleukin-1β (5). Together, these observations suggest that EL may be proatherogenic.

The importance of glycosylation in glycoprotein structure and function is indisputable (15). *N*-Glycosylation, one of the most common posttranslational modifications occurring in eukaryotic cells, is involved in protein folding, intracellular trafficking, and the secretion of proteins in their biologically active conformations (16). In general, *N*-linked glycans confer stability to the glycoprotein to which they are attached, increase plasma residence times, and provide steric protection from proteases and nonspecific interactions (17). *N*-Linked oligosaccharides can also modify protein binding through carbohydrate-based ligand-receptor interactions (17). Recent studies have also shown that *N*-glycosylation dramatically affects the activities of several proteins and enzymes, including human gastric lipase (18) and the HDL receptor scavenger receptor class B type I (19).

N-Glycosylation occurs at the Asn-Xxx-Ser/Thr consensus sequence of a protein; however, only 70–90% of these sites are typically glycosylated (20). It was recently shown that in human EL, four of the five potential *N*-linked glycosylation sites are used in vivo, giving rise to an enzyme bearing predominantly endoH-resistant (or "complex-type") *N*-glycans at positions 62, 118, 375, and 473 (12). These glycans account for ~18% of the total EL mass.

In a previous study using triolein/egg phosphatidylcholine glycerol-stabilized emulsions, the individual *N*-glycans in EL had varying effects on secretion and lipolytic activity

(12). The aim of the current study was to determine precisely how these individual *N*-glycans affect the phospholipase activity of EL in much more physiologically relevant HDL substrates that contain either apoE or apoA-I as the sole apolipoprotein.

The ability of apoE to protect against atherosclerosis is well established (21). Three isoforms of apoE, apoE2, apoE3, and apoE4, which have cysteine-arginine interchanges at residues 112 and 158, have been identified in human plasma (21). The cysteine residues at positions 112 and 158 are involved in disulfide bond and salt bridge formation. Substitution of these residues with arginine has structural and functional consequences on the stability and receptor binding affinity of apoE and on its association with lipoproteins. The majority of plasma apoE in normolipidemic subjects is associated with HDLs that do not contain apoA-I and that range in size from 9.0 to 18.5 nm in diameter (22). As the development of new therapies that inhibit cholesteryl ester transfer protein activity and increase HDL levels is likely to generate large HDL particles that are enriched in apoE (23), it is of major importance to understand how the metabolism of these particles is regulated.

Although previous studies from this laboratory have shown that apoA-I regulates the kinetics of wild-type (i.e., fully glycosylated) EL-mediated phospholipid hydrolysis in reconstituted high density lipoprotein (rHDL) (24), nothing is known about apoE-containing HDL. The present study uses homogenous preparations of rHDL that contain apoE2, apoE3, apoE4, or apoA-I as the only apolipoprotein and variably deglycosylated EL mutants (Fig. 1B) to determine how individual *N*-glycans affect the ability of EL to interact with and hydrolyze the phospholipids in rHDL of varying apolipoprotein composition. To demonstrate the physiological relevance of apoE-containing rHDLs as substrates for EL, comparisons with apoE-rich native HDLs are also presented.

EXPERIMENTAL PROCEDURES

Isolation of apoA-I

HDLs were obtained by sequential ultracentrifugation ($1.07 < d < 1.21$ g/ml) of pooled, expired, autologously donated human plasma (Gribbles Pathology, Adelaide, Australia). Delipidation of HDL, followed by anion-exchange chromatography of the resulting apoHDL (fast-protein liquid chromatography: Q-Sepharose Fast Flow; GE Healthcare, Uppsala, Sweden), afforded apoA-I, which appeared as a single band when subjected to electrophoresis on a homogeneous, 20% SDS-polyacrylamide PhastGel (GE Healthcare) and Coomassie staining (25).

Production of recombinant apoE2, apoE3, and apoE4

ApoE2, apoE3, and apoE4 were obtained by bacterial overexpression in *Escherichia coli* strain BL21 (26). Vectors containing human apoE2, apoE3, and apoE4 cDNA were kindly provided by Dr. Karl Weisgraber (Gladstone Institute of Neurological Disease, University of California, San Francisco, CA). Each apoE isoform was purified by gel permeation chromatography on Sephacryl S-300 (GE Healthcare) and appeared as a single band after electrophoresis on a homogeneous 20% SDS-polyacrylamide gel and Coomassie staining (27).

Preparation of LCAT

LCAT was isolated from pooled, expired, autologously donated human plasma as described previously (28). LCAT activity was measured using discoidal rHDL comprising apoA-I, POPC (Avanti Polar Lipids, Alabaster, AL), unesterified cholesterol (UC; Sigma), and a tracer amount of [1*R*,2*R*-^{3}H]cholesterol ([^{3}H]UC) (Amersham) as the substrate (29). The assay was linear provided that <30% [^{3}H]UC was esterified. The activities of the LCAT preparations used in this study ranged from 7,025 to 7,556 nmol cholesteryl ester (CE) generated/ml LCAT/h.

Preparation of spherical (E2)rHDL, (E3)rHDL, (E4)rHDL, and (A-I)rHDL

Discoidal rHDLs containing POPC, UC, and apoE2, apoE3, apoE4, or apoA-I were prepared according to the cholate dialysis method (30). Spherical rHDLs were prepared by incubating the discoidal rHDLs with LDL and LCAT (31). The resulting spherical rHDLs contained CE as the sole core lipid and are herein described as (E2)rHDL, (E3)rHDL, (E4)rHDL, and (A-I)rHDL. All rHDLs were dialyzed extensively (3 × 1 liter) against 0.01 M TBS (pH 7.4) containing 0.15 M NaCl, 0.005% (w/v) EDTA-Na_2, and 0.006% (w/v) NaN_3 before use.

Isolation of apoE-rich HDL

ApoE-rich HDLs were obtained by heparin-Sepharose chromatography of pooled, autologously donated human plasma samples according to the method of Thuren et al. (32). Fractions were collected and analyzed for apoE by ELISA. The apoE-rich HDL fractions were then pooled and dialyzed against TBS. The cholesterol/apoE molar ratio of the resulting preparations was 168:1. This is comparable to what has been reported elsewhere (33). The average concentration of apoE in these preparations was 93 μg/ml.

Expression of wild-type EL

Wild-type EL was transiently expressed in HEK-293 cells. To obtain cell-free enzyme preparations, heparin was added to the medium. Expression was confirmed by mRNA extraction followed by real-time PCR, as described previously (12, 24).

The medium was collected and clarified by centrifugation at 2,000 rpm for 10 min and frozen in 1 ml aliquots at −80°C. The phospholipase activity of the cell-free wild-type EL was determined by incubating the enzyme (40 μl) with spherical (A-I)rHDL (0.5 mM final phospholipid concentration) at 37°C for 2 h and measuring the formation of NEFA mass. The preparation used in this study generated 224 nmol NEFA/ml EL/h.

For the studies using cell-bound enzyme, transfected cells were placed on 96-well tissue culture plates (35,000 cells/well) and maintained in 100 μl of medium. Comparable numbers of nontransfected cells were used as negative controls.

Expression of glycan-deficient mutants of EL

Site-directed mutagenesis of the EL glycosylation sequences (Asn-Xxx-Ser/Thr), replacing asparagine (N) with alanine (A) at positions 62, 118, 375, and 473, was performed as described (12). The nucleotide sequence of each construct was confirmed by DNA sequencing. Cell-free preparations of the glycan-deficient mutants, designated EL N62A, EL N118A, EL N375A, and EL N473A, were transiently expressed in HEK-293 cells in the presence of heparin (12, 24). The phospholipase activities of the mutants were determined as described for wild-type EL. The EL N62A, N118A, N375A, and N473A used in this study generated 17, 140, 15, and 92 nmol NEFA/ml EL/h, respectively.

Kinetic studies

Varying concentrations of (E2)rHDL, (E3)rHDL, (E4)rHDL, and (A-I)rHDL (0.2–1.0 mM final phospholipid concentration) were incubated individually with a constant amount of cell-free EL and BSA (final concentration, 40 mg/ml) in a final incubation volume of 40 μl. All incubations were carried out in stoppered plastic tubes in a shaking-water bath maintained at 37°C. Details of the individual incubations are described in the legends to the figures. The mixtures were placed on ice when the incubations were complete. The extent of phospholipid hydrolysis was determined by quantification of NEFA mass using a NEFA C enzymatic test kit (WAKO Pure Chemical Industries, Ltd., Osaka, Japan), 96-well microtiter plates, and a microplate reader (Tecan Sunrise, Durham, NC) (34). The kinetic studies were all conducted under conditions that gave <20% phospholipid hydrolysis. Experiments with cell-bound EL were performed in an analogous manner on 96-well plates (final incubation volume, 200 μl).

Other techniques

All chemical analyses were carried out on a Roche Diagnostics/Hitachi 902 automatic analyzer (Roche Diagnostics GmbH, Mannheim, Germany). Phospholipid and UC concentrations were determined enzymatically (35, 36). A Roche Diagnostics Kit was used for total cholesterol assays. CE concentrations were calculated as the difference between the total cholesterol and UC concentrations. A bicinchoninic acid protein assay was used to determine apoA-I and apoE concentrations (37). Spherical rHDL size was determined by electrophoresis on 3–40% nondenaturing polyacrylamide gradient gels (38). EL mass was determined by triplicate measurements using an ELISA (12).

Statistical analysis

The kinetic parameters V_{max} and K_m(app) were derived by nonlinear regression analysis using GraphPad Prism version 4.0b for Macintosh (Graph-Pad Software, Inc., San Diego, CA) and the Michaelis-Menten equation $Y = V_{max}X/(K_m + X)$, where V is the rate of EL-mediated phospholipid hydrolysis expressed as μmol NEFA formed/mg EL/h and X is the concentration of phospholipid in the substrate (mM). The Lineweaver-Burk double-reciprocal plots shown in the figures are for visualization only and were not used to determine kinetic parameters. All measurements were made in triplicate, and the data shown are means of at least two independent experiments. Two-way ANOVA (GraphPrism) was used to determine whether differences between data sets were significant, with significance set at $P < 0.05$.

RESULTS

Physical properties of spherical (E2)rHDL, (E3)rHDL, (E4)rHDL, and (A-I)rHDL

Spherical (E2)rHDL, (E3)rHDL, (E4)rHDL, and (A-I)rHDL were prepared as described in Experimental Procedures. The rHDLs were comparable in their protein-to-lipid ratio (**Table 1**). (E2)rHDL, (E3)rHDL, and (E4)rHDL were all similar in size, ~25% larger in diameter than (A-I)rHDL.

TABLE 1. Physical properties of spherical rHDLs

Spherical rHDL	Stoichiometry[a]				Stokes' Diameter[b]
	Protein	PL	Unesterified Cholesterol	Cholesteryl Ester	
	mol/mol				*nm*
(E2)rHDL	1.0	108.1	23.3	15.6	11.3
(E3)rHDL	1.0	86.9	12.4	21.3	11.5
(E4)rHDL	1.0	104.5	22.5	15.2	11.6
(A-I)rHDL	1.0	65.2	3.8	14.6	9.2

PL, phospholipid; rHDL, reconstituted high density lipoprotein. Spherical (E2)rHDL, (E3)rHDL, (E4)rHDL, and (A-I)rHDL were prepared by incubating the corresponding discoidal rHDL with LCAT and LDL, as described in Experimental Procedures.

[a] Stoichiometries were calculated from the means of triplicate determinations, which varied by <10%.

[b] rHDL sizes were determined by nondenaturing 3–40% polyacrylamide gradient gel electrophoresis and Coomassie staining.

Effect of *N*-glycosylation on the secretion of EL

Removal of the *N*-glycosylation site at residue 62 dramatically reduced secretion from HEK-293 cells, as described previously (12). A more moderate reduction in secretion was observed for mutation of the conserved C-terminal residue at position 375. Replacement of the two nonconserved asparagine residues at positions 118 and 473 to alanine did not have an appreciable effect on enzyme secretion (Fig. 1B).

Kinetics of wild-type EL-mediated phospholipid hydrolysis in rHDL and native apoE-rich HDL

Increasing concentrations of spherical (E2)rHDL, (E3)rHDL, (E4)rHDL, (A-I)rHDL, and native apoE-rich HDL were incubated individually with a constant amount of wild-type EL. The rate of phospholipid hydrolysis was assessed as the formation of NEFA mass (34). Nonlinear regression analysis of the rate of phospholipid hydrolysis as a function of rHDL phospholipid concentration is shown in **Fig. 2** (solid lines). The kinetics of phospholipid hydrolysis by wild-type EL in (E2)rHDL, (E3)rHDL, and (E4)rHDL were not significantly different from those obtained for (A-I)rHDL, as judged by two-way ANOVA. The apoE isoforms had a minor effect on the rate of phospholipid hydrolysis, with (E3)rHDL < (E2)rHDL ~ (E4)rHDL [$P < 0.05$ for (E2)rHDL vs. (E3)rHDL]. The rate of phospholipid hydrolysis for the native apoE-rich HDL (Fig. 2, dotted lines) was essentially identical to that of (E3)rHDL and lower than what was obtained for (E2)rHDL and (E4)rHDL.

The V_{max} of phospholipid hydrolysis for (E2)rHDL, (E4)rHDL, and (A-I)rHDL ranged from 14.3 to 16.9 μmol NEFA/mg EL/h, compared with 11.2 ± 0.8 μmol NEFA/mg EL/h for (E3)rHDL (**Table 2**). The K_m(app) values for (E2)rHDL, (E4)rHDL, and (A-I)rHDL were comparable and slightly lower for (E3)rHDL. The catalytic efficiency of phospholipid hydrolysis was comparable for all rHDLs. Although the V_{max} for the native apoE-rich HDL (10.3 μmol NEFA/mg EL/h) was comparable to that for (E3)rHDL, the K_m(app) was significantly lower than what was observed for the apoE-containing rHDL. This is indicative of a higher binding affinity of the enzyme for the naturally occurring substrate compared with rHDL.

Kinetics of EL N62A-mediated phospholipid hydrolysis in rHDL and native apoE-rich HDL

The glycan-deficient mutant N62A dramatically increased EL-mediated phospholipid hydrolysis relative to wild-type EL for all of the rHDLs (**Fig. 3**, solid lines). The

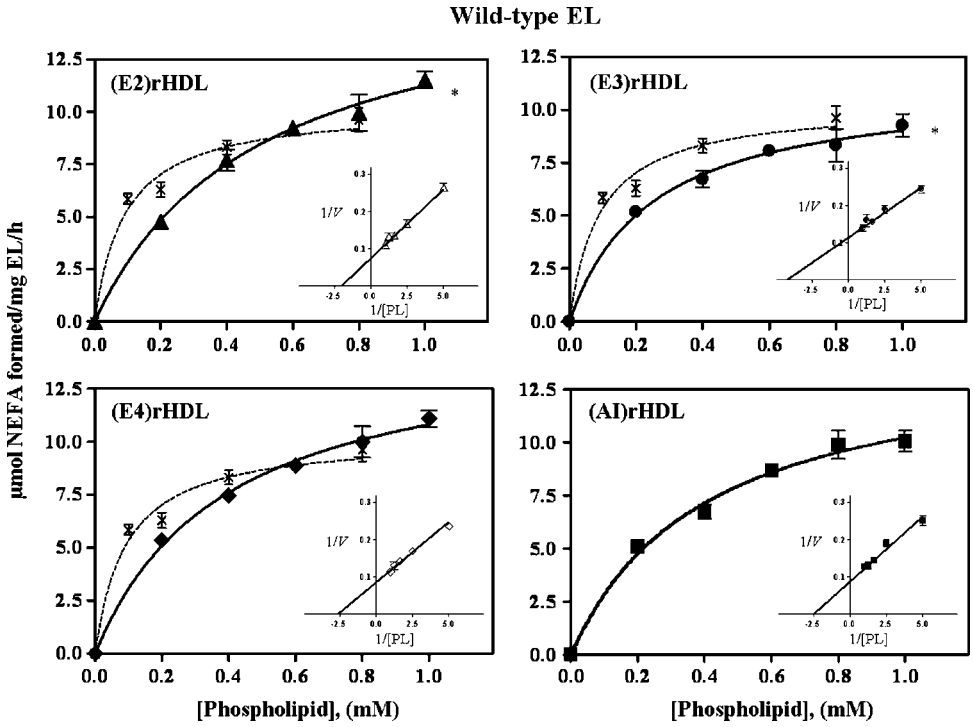

Fig. 2. Kinetics of wild-type EL-mediated phospholipid hydrolysis in (E2)rHDL (for reconstituted high density lipoprotein), (E3)rHDL, (E4)rHDL, (A-I)rHDL, and native apolipoprotein E (apoE)-rich HDL. Varying amounts of rHDL (0.1–1.0 mM final phospholipid concentration), a constant amount of EL (8 μl of a preparation that generated 224 nmol NEFA/ml EL/h), and BSA (final concentration, 40 mg/ml), in a final incubation volume of 40 μl, were maintained at 37°C for 2 h. The rates of phospholipid hydrolysis in (E2)rHDL, (E3)rHDL, (E4)rHDL, and (A-I)rHDL as a function of substrate concentration are shown in individual panels. The dotted lines show the rate of phospholipid hydrolysis in native apoE-rich HDL. Each data point is the mean ± SEM of triplicate determinations from at least two independent experiments, with <10% variation. Insets show Lineweaver-Burk double-reciprocal plots of the rHDL kinetic data. * $P < 0.05$ for (E2)rHDL versus (E3)rHDL.

kinetics of phospholipid hydrolysis were comparable for the (E2)rHDL, (E3)rHDL, and (E4)rHDL but significantly different for the (A-I)rHDL [$P < 0.05$ for (A-I)rHDL vs. (E2)rHDL, (E3)rHDL, and (E4)rHDL].

EL N62A hydrolyzed the phospholipids in native apoE-rich HDL at a rate that was ~3- to 5-fold greater than what was observed for the apoE-containing rHDL (Fig. 3, dotted lines). The mutant enzyme also had higher affinity for the native apoE-rich HDL than for the apoE-containing rHDL. As the phospholipids in the native apoE-rich HDL were hydrolyzed so rapidly, it was not possible to obtain reliable kinetic parameters. This result suggests that the native HDLs most likely contain one or more minor constituents that markedly enhance the access of the substrate phospholipids to the active site of the mutant enzyme. It also highlights the importance of *N*-glycosylation in determining the substrate specificity of EL.

The V_{max} values of phospholipid hydrolysis for (E2)rHDL, (E3)rHDL, and (E4)rHDL of 104 ± 20, 67 ± 9.5, and 70 ± 9.1 μmol NEFA/mg EL/h, respectively, were up to 6-fold greater than those observed for wild-type EL (Table 2). The V_{max} of phospholipid hydrolysis for (A-I)rHDL was 38 ± 2.4 μmol NEFA/mg EL/h, 3-fold higher than for wild-type EL. The K_m(app) values for (E2)rHDL, (E3)rHDL, and (E4)rHDL were comparable to, and not significantly different from, those obtained with wild-type EL. However, the K_m(app) of EL N62A for (A-I)rHDL was 1 order of magnitude less than that obtained for wild-type EL, indicating a significant increase in the affinity of the mutant enzyme for this substrate. The V_{max}/K_m(app) ratios for phospholipid hydrolysis of the apoE-containing spherical rHDL substrates by EL N62A were 4- to 6-fold higher than for wild-type EL. The catalytic efficiency of phospholipid hydrolysis for (A-I)rHDL was 4- to 7-fold higher than for the apoE-containing rHDL and 26-fold higher than for the phospholipid hydrolysis of (A-I)rHDL by wild-type EL.

Kinetics of EL N118A-mediated phospholipid hydrolysis in rHDL and native apoE-rich HDL

The rate of phospholipid hydrolysis mediated by the glycan-deficient mutant N118A was less than half that of wild-type EL for all of the rHDLs (**Fig. 4**, solid lines). As judged by two-way ANOVA, the rate of phospholipid hydrolysis was not significantly different for (E2)rHDL, (E4)rHDL, or (A-I)rHDL. However, the rate of phospholipid hydrolysis for (E3)rHDL was lower than for the other rHDLs (Fig. 4) [$P < 0.05$ for (E3)rHDL vs. (A-I)rHDL and (E2)rHDL]. As with the EL N62A mutant, EL N118A had a much higher affinity for the native apoE-rich HDL than for the apoE-containing rHDL. It also hydrolyzed the

TABLE 2. Kinetic parameters of wild-type and mutant EL-mediated PL hydrolysis in spherical rHDLs and native apoE-rich HDL

Spherical rHDL	Wild-Type EL			EL N62A			EL N118A			EL N473A		
	V_{max}	K_m(app)	Catalytic Efficiency	V_{max}	K_m(app)	Catalytic Efficiency	V_{max}	K_m(app)	Catalytic Efficiency	V_{max}	K_m(app)	Catalytic Efficiency
	μmol NEFA/mg EL/h	*mM PL*	V_{max}/K_m (app)	*μmol NEFA/mg EL/h*	*mM PL*	V_{max}/K_m (app)	*μmol NEFA/mg EL/h*	*mM PL*	V_{max}/K_m (app)	*μmol NEFA/mg EL/h*	*mM PL*	V_{max}/K_m (app)
(A-I)rHDL	14.3 ± 1.2	0.4 ± 0.08	36	38 ± 2.4	0.04 ± 0.03	950	5.6 ± 0.2	0.1 ± 0.02	56	5.5 ± 0.30	0.2 ± 0.04	29
(E2)rHDL	16.9 ± 1.7	0.5 ± 0.1	34	104 ± 20	0.8 ± 0.3	137	6.5 ± 0.3	0.1 ± 0.03	46	6.7 ± 0.46	0.3 ± 0.06	20
(E3)rHDL	11.2 ± 0.8	0.3 ± 0.06	37	67 ± 9.5	0.3 ± 0.1	239	5.1 ± 0.4	0.1 ± 0.06	36	4.0 ± 0.26	0.1 ± 0.04	15
(E4)rHDL	15.0 ± 1.1	0.4 ± 0.07	38	70 ± 9.1	0.4 ± 0.1	175	6.1 ± 0.4	0.1 ± 0.04	44	12.0 ± 2.0	1.0 ± 0.3	13
ApoE-rich HDL	10.3 ± 0.5	0.09 ± 0.02	34	ND	ND	ND	ND	ND	ND	ND	ND	ND

ApoE, apolipoprotein E; EL, endothelial lipase. Varying concentrations of spherical rHDLs and native apoE-rich HDL (0.1–1.0 mM final PL concentration) were incubated with a constant amount of EL, as described in the legends to Figs. 2–5 and in Experimental Procedures. The resulting NEFAs were measured by a colorimetric mass assay as described in Experimental Procedures. Kinetic parameters were derived by nonlinear regression analysis of the rate of PL hydrolysis as a function of HDL concentration (see Figs. 2–5).

phospholipids in these preparations at a greater rate than what was observed for the apoE-containing rHDL (Fig. 4, dotted lines).

The V_{max} of phospholipid hydrolysis for (E2)rHDL, (E3)rHDL, (E4)rHDL, and (A-I)rHDL varied between 5.1 and 6.5 μmol NEFA/mg EL/h (Table 2). In all cases, the K_m(app) was 0.1 mM phospholipid, which is significantly lower than the values obtained with wild-type EL. This is indicative of an increased binding affinity of EL for all rHDL substrates upon removal of the glycosylation site at position 118. The catalytic efficiencies were comparable for all spherical rHDL substrates and either the same or slightly greater than those obtained for wild-type EL.

Kinetics of EL N473A- and EL N375A-mediated phospholipid hydrolysis in rHDL

As was the case for EL N118A, the rate of phospholipid hydrolysis for (E2)rHDL, (E3)rHDL, and (A-I)rHDL by the glycan-deficient mutant N473A was less than half that of wild-type EL (**Fig. 5**, Table 2). As judged by two-way ANOVA, the rate of phospholipid hydrolysis was significantly greater for (E4)rHDL compared with the other rHDLs [$P < 0.05$ for (E4)rHDL vs. (E2)rHDL, (E3)rHDL, and (A-I)rHDL] but was unchanged relative to wild-type EL (Fig. 2). The kinetics of phospholipid hydrolysis for (E2)rHDL versus (A-I)rHDL were comparable, whereas (E3)rHDL showed the least phospholipid hydrolysis [$P < 0.05$ for (E3)rHDL vs. (E2)rHDL and (A-I)rHDL].

The K_m(app) for (E4)rHDL was particularly high, indicating that EL N473A has a lower binding affinity for these particles than wild-type EL. Conversely, both the lowest V_{max}, 4.0 ± 0.3 μmol NEFA/mg EL/h, and the lowest K_m(app), 0.1 ± 0.04 mM phospholipid, were attained for (E3)rHDL, suggesting that EL N473A has a higher binding affinity for this rHDL substrate. The V_{max} and K_m(app) data for (E2)rHDL and (A-I)rHDL were similar. Apart from (E4)rHDL, all other rHDLs displayed significantly lower K_m(app) values than those obtained for wild-type EL. The highest catalytic efficiency for phospholipid hydrolysis was obtained for (A-I)rHDL, followed by (E2)rHDL. The catalytic efficiencies for (E3)rHDL and (E4)rHDL were comparable. The V_{max}/K_m(app) ratios for each of the rHDL substrates were appreciably reduced compared with those obtained for wild-type EL, EL N62A, and EL N118A.

The V_{max} of phospholipid hydrolysis for EL N375A was comparable for all of the rHDLs and approximately one-third of what was obtained for wild-type EL (data not shown). Nonlinear regression analysis of the rate of phospholipid hydrolysis and two-way ANOVA analysis demonstrated that the kinetics of phospholipid hydrolysis were not significantly different for (E2)rHDL, (E3)rHDL, (E4)rHDL, or (A-I)rHDL (data not shown).

Kinetics of cell-bound, wild-type EL-mediated phospholipid hydrolysis in rHDL

Given that a proportion of EL is cell-associated in vivo (39), it was important to establish whether immobilized EL could hydrolyze HDL phospholipids at a rate comparable to what was observed for cell-bound EL. This was achieved

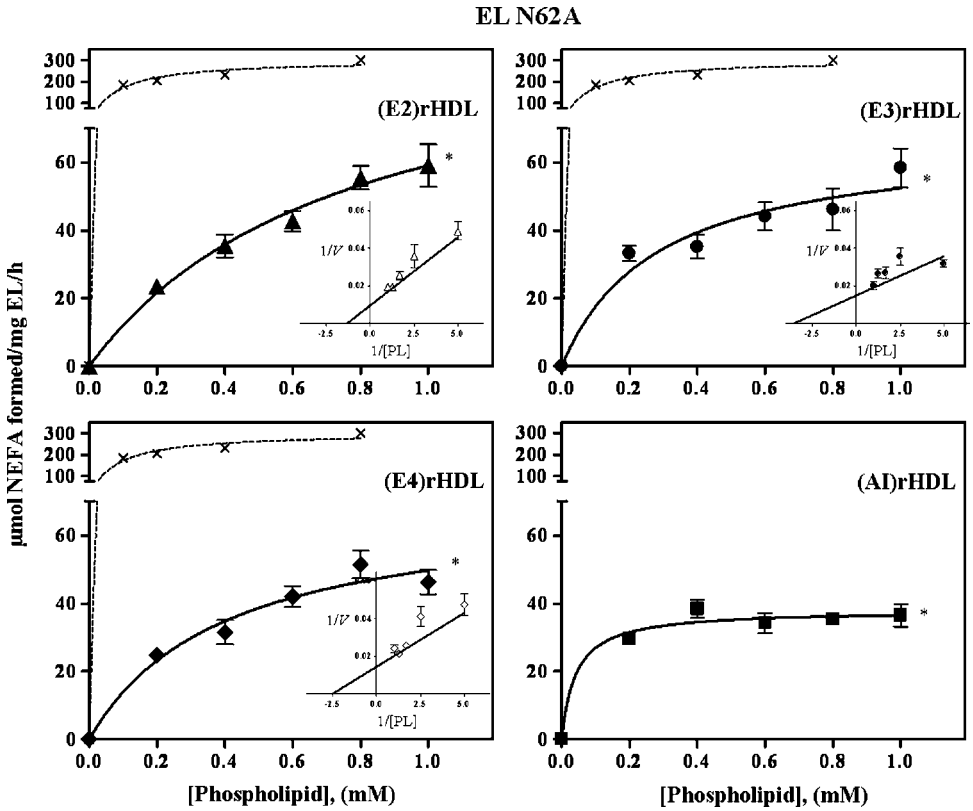

Fig. 3. Kinetics of EL N62A-mediated phospholipid hydrolysis in (E2)rHDL, (E3)rHDL, (E4)rHDL, (A-I)rHDL, and native apoE-rich HDL. Varying amounts of rHDL (0.1–1.0 mM final phospholipid concentration), a constant amount of EL (14.6 µl of a preparation that generated 17 nmol NEFA/ml EL/h), and BSA (final concentration, 40 mg/ml), in a final incubation volume of 40 µl, were maintained at 37°C for 2 h. The rates of phospholipid hydrolysis in (E2)rHDL, (E3)rHDL, (E4)rHDL, and (A-I)rHDL as a function of substrate concentration are shown in individual panels. The dotted lines show the rate of phospholipid hydrolysis in native apoE-rich HDL. Each data point is the mean ± SEM of triplicate determinations from at least two independent experiments, with <10% variation. Insets show Lineweaver-Burk double-reciprocal plots of the kinetic data for (E2)rHDL, (E3)rHDL, and (E4)rHDL. The Lineweaver-Burk plot for (A-I)rHDL is not shown because the V_{max} of phospholipid hydrolysis was reached at a low concentration of substrate. * $P < 0.05$ for (A-I)rHDL versus (E2)rHDL, (E3)rHDL, and (E4)rHDL.

by incubating increasing concentrations of spherical (E2)rHDL, (E3)rHDL, (E4)rHDL, and (A-I)rHDL with a constant amount of cell-bound, wild-type EL and measuring NEFA formation. The results showed that cell-bound EL hydrolyzed the phospholipids in the apoE-containing rHDLs and (A-I)rHDL to a similar extent (**Table 3**). This result is comparable to what was obtained for cell-free EL (Table 2).

DISCUSSION

The results of this study show that the removal of individual *N*-glycans from EL has striking effects on its secretion, on its interaction with physiologically relevant substrates, and on its phospholipase activity. This was achieved by mutating the asparagine residue of four of the *N*-linked glycosylation sites in EL to alanine to generate mutants that lacked single *N*-glycans. The rationale for undertaking this study is that it has become increasingly apparent in recent years that glycosylation plays a key role in the secretion, structure, and function of a wide range of plasma enzymes. Although it is generally believed that defective or reduced glycosylation attenuates enzyme activity, this study provides compelling evidence that this is not necessarily the case, with the phospholipase activity of EL increasing dramatically after the removal of one of its *N*-glycans.

The effects of *N*-linked glycosylation on EL secretion are somewhat variable and appear to be dependent on cell type. In this study, removal of the conserved glycosylation site at position 62 dramatically reduced the secretion of EL from HEK-293 cells. This is consistent with what has been reported previously for EL (12) and for the corresponding conserved glycosylation sites in human LPL and HL (40–42). Site-directed mutagenesis of the residues at positions 118, 375, and 473 to either alanine or glutamine has been described as having no effect on the secretion of EL from either COS or HEK-293 cells (12). However, in this study, we observed a reduction in the secretion of EL from HEK-293 cells to about half that of wild-type EL when the asparagine residue at position 375 was mutated to alanine.

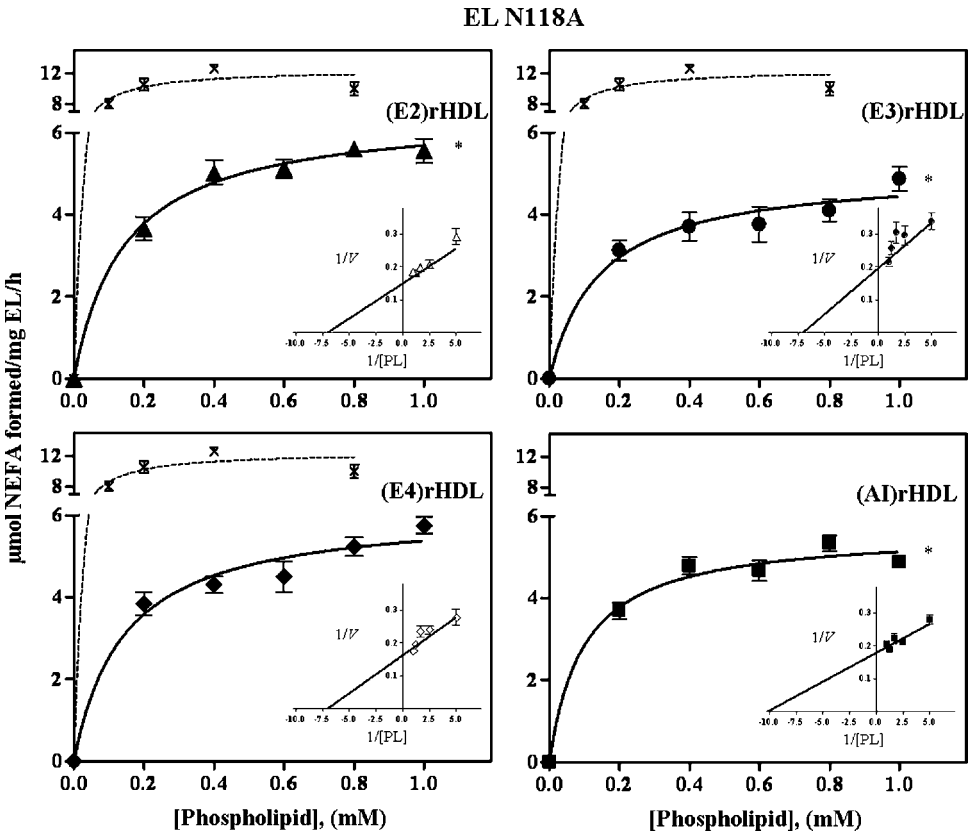

Fig. 4. Kinetics of EL N118A-mediated phospholipid hydrolysis in (E2)rHDL, (E3)rHDL, (E4)rHDL, (A-I)rHDL, and native apoE-rich HDL. Varying amounts of rHDL (0.1–1.0 mM final phospholipid concentration), a constant amount of EL (12 µl of a preparation that generated 140 nmol NEFA/ml EL/h), and BSA (final concentration, 40 mg/ml), in a final incubation volume of 40 µl, were maintained at 37°C for 2 h. The rates of phospholipid hydrolysis in (E2)rHDL, (E3)rHDL, (E4)rHDL, and (A-I)rHDL as a function of substrate concentration are shown in individual panels. The dotted lines show the rate of phospholipid hydrolysis in native apoE-rich HDL. Each data point is the mean ± SEM of triplicate determinations from two independent experiments, with <10% variation. Insets show Lineweaver-Burk double-reciprocal plots of the rHDL kinetic data. * $P < 0.05$ for (E3)rHDL versus (A-I)rHDL and (E2)rHDL.

Interestingly, removal of the homologous residue in human HL did not compromise its secretion from Chinese hamster ovary cells (42) but did reduce its secretion from COS-7 cells (43). Mutation of the related conserved residue in human LPL had no effect on secretion from COS cells (40, 41, 43).

The present results also show that the four *N*-glycans in EL have diverse effects on its ability to bind to, or recognize, HDL subpopulations of varying apolipoprotein composition. The individual glycosylation sites at asparagine 118, 375, and 473 are essential for the full complement of EL phospholipase activity, with the loss of any individual glycan reducing the enzyme activity to less than half that of the fully glycosylated form. In a recent study, however, increased enzyme activity was observed for EL N118A with LDL as well as HDL_2, highlighting the potential role of *N*-linked glycosylation in determining substrate specificity (44). Whether these results reflect a change in the active conformation of the enzyme or are based on steric considerations, such as regulating access of the substrate to the active site, will require further investigation.

The most striking observation we have made is that *N*-glycosylation of the conserved N-terminal site at position 62, although essential for secretion, may sterically hinder access of the substrate to the active site, such that its removal markedly increases the phospholipase activity of EL. To the best of our knowledge, this is the first case in which removal of a single *N*-glycosylation site has resulted in such a dramatic (6-fold) increase in the catalytic activity of an enzyme.

The current results have provided unique insights into the interaction of EL with different types of HDL. Recent studies have demonstrated that the C-terminal domain of EL regulates its ability to bind and hydrolyze HDL lipids, whereas the lid, which covers the catalytic site in the N-terminal domain, mediates lipid substrate specificity (45). If the activation of EL by apoE-containing HDL involves protein-protein interactions, as described for HL (32), then our findings, which show that wild-type EL hydrolyzes the phospholipids in apoE- and apoA-I-containing rHDLs, as well as native apoE-rich HDL, equally well, suggest that the C-terminal domain of EL interacts similarly with these

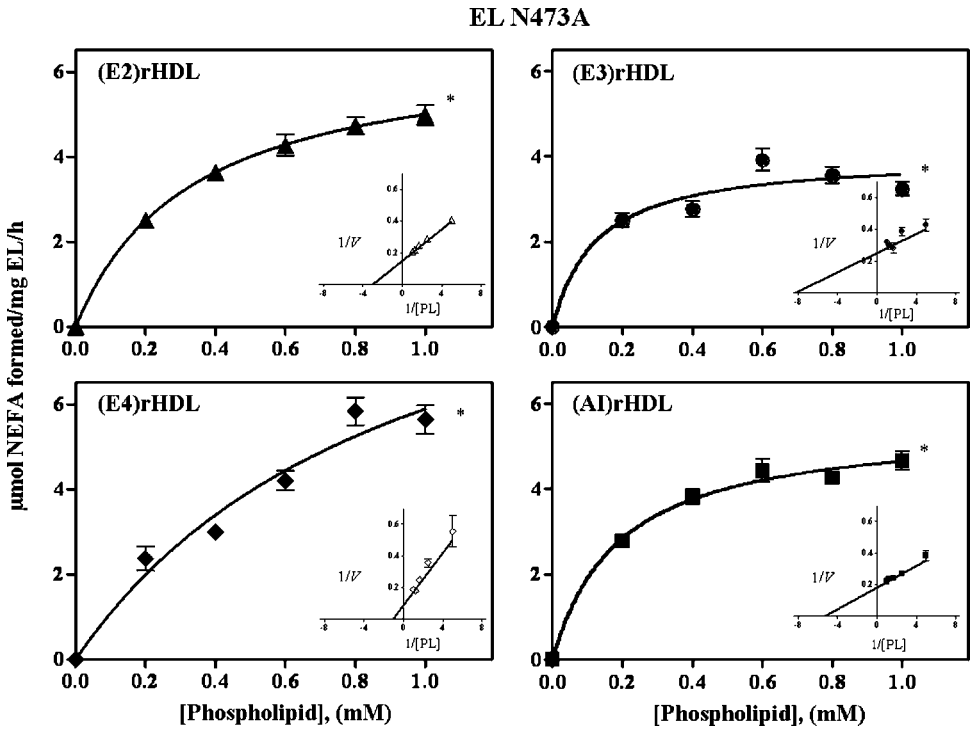

Fig. 5. Kinetics of EL N473A-mediated phospholipid hydrolysis in (E2)rHDL, (E3)rHDL, (E4)rHDL, and (A-I)rHDL. Varying amounts of rHDL (0.1–1.0 mM final phospholipid concentration), a constant amount of EL (12 µl of a preparation that generated 92 nmol NEFA/ml EL/h), and BSA (final concentration, 40 mg/ml), in a final incubation volume of 40 µl, were maintained at 37°C for 2 h. The rates of phospholipid hydrolysis in (E2)rHDL, (E3)rHDL, (E4)rHDL, and (A-I)rHDL as a function of substrate concentration are shown in individual panels. Each data point is the mean ± SEM of triplicate determinations from at least two independent experiments, with <10% variation. Insets show Lineweaver-Burk double-reciprocal plots of the kinetic data. * $P < 0.05$ for (E2)rHDL versus (E3)rHDL and (E4)rHDL, (E3)rHDL versus (E4)rHDL, and (A-I)rHDL versus (E3)rHDL and (E4)rHDL.

particles. This is consistent with apoE and apoA-I sharing a common two-domain conformation and key structural elements, such as 22 amino acid residue amphipathic α-helical repeats (46).

This study also establishes that for cell-free as well as cell-bound EL, the rate of wild-type (i.e., fully glycosylated) EL-mediated phospholipid hydrolysis is essentially independent of the apoE isoform content of the substrate, with small but significant differences being apparent only between (E2)rHDL and (E3)rHDL. The result for cell-free EL is in contrast to what has been reported for cell-free HL, in which phospholipid hydrolysis is greater in apoE-containing HDLs than in apoA-I-containing HDL. In further contrast to what was found in this study, the ability of HL to hydrolyze the phospholipids in apoE-containing rHDLs was isoform-dependent (27, 32). Together, these results suggest that EL and HL may interact with HDL via different mechanisms.

TABLE 3. Kinetic parameters of cell-bound wild-type EL-mediated PL hydrolysis in spherical rHDLs

	Wild-Type EL	
Spherical rHDL	V_{max}	K_m(app)
	µmol NEFA/10^6 cells EL/h	*mM PL*
(A-I)rHDL	2.3 ± 0.5	0.1 ± 0.1
(E2)rHDL	4.7 ± 2.3	0.1 ± 0.2
(E3)rHDL	6.6 ± 2.0	0.2 ± 0.2
(E4)rHDL	10.4 ± 8.3	0.8 ± 0.9

Varying concentrations of spherical rHDLs (0.1–0.8 mM final PL concentration) were incubated with a constant amount of cell-bound EL, and the resulting NEFAs were measured as described in Experimental Procedures. The values represent means ± SEM of triplicate determinations. Kinetic parameters were derived by nonlinear regression analysis of the rate of PL hydrolysis as a function of HDL concentration.

Our results also show that, irrespective of which sites are glycosylated, EL has a higher affinity for the phospholipids in (E3)rHDL than for the phospholipids in either (E2)rHDL or (E4)rHDL (Table 2). This is consistent with what has been observed for HL (27). When considered in light of the observation that phospholipid head group and acyl chain packing is less ordered in (E3)rHDL compared with (E2)rHDL and (E4)rHDL (27), it follows that the phospholipids in spherical (E3)rHDL may be able to access the active site of EL more readily than the phospholipids in either (E2)rHDL or (E4)rHDL (27).

One of the most important outcomes of this study is the finding that removal of the *N*-glycosylation site at position 62 of EL markedly increased the rate of phospholipid hydrolysis in apoE-containing rHDLs, (A-I)rHDL, and na-

tive apoE-rich HDL. Mutation of the asparagine residue at position 62 also increased the catalytic efficiency of EL-mediated phospholipid hydrolysis up to 7-fold for apoE-containing rHDLs and 26-fold for (A-I)rHDL. The latter result was primarily attributable to the significantly higher affinity of this EL mutant for the (A-I)rHDL. This result is in contrast to what has been reported previously for the triglyceride lipase activity of glycan-deficient EL mutants determined using glycerol-stabilized triolein emulsions as the substrate (12). In that study, triglyceride lipase activity was increased only slightly for the EL N62A mutant. This difference highlights the importance of using physiologically relevant substrates in studies of this type.

A comparative study of native apoE-rich HDL versus apoE-containing rHDLs revealed that wild-type EL hydrolyzes the phospholipids in both types of HDL to the same extent. In contrast to wild-type EL, the glycan-deficient mutants N62A and N118A hydrolyzed the phospholipids in native apoE-rich HDL more rapidly than in apoE-containing rHDLs. This is possibly a reflection of the presence of different phospholipids, as well as apolipoproteins other than apoE, in the apoE-rich HDL and emphasizes the importance of *N*-glycosylation in determining substrate specificity.

To gain insight into the underlying reason for the enhanced lipolytic activity of the EL N62A mutant, it is important to know where in the EL molecule this residue is located. A model of the three-dimensional structure of human LPL (7, 8, 47), which is based on the X-ray crystal structure of human pancreatic lipase (10, 11), has shown that the conserved N-terminal glycosylation site at position 43 is situated in the vicinity of the catalytic site (47). As EL shows a high degree of sequence homology with LPL, this suggests that the glycan at position 62 may also be in close proximity to the catalytic site. As *N*-glycans occupy a large space, ~3 nm in diameter (17, 48), it follows that this glycan may sterically hinder access of the substrate to the active site of the enzyme, so that its removal increases the activity. This explanation could also account for the increased catalytic activity that is observed when the conserved asparagine residue at position 57 in rat HL is removed (49).

It is extremely rare to observe an increase in enzyme activity upon removal of a single *N*-glycan. In most cases, this has been shown to markedly reduce protein function, enzyme-substrate interactions, and enzyme activity (18, 19), as we have shown for the glycan-deficient EL N118A, N473A, and N375A mutants. One exception is the increased activity of RNase A, which is an unglycosylated variant of RNase B (17, 50). Pritchard and colleagues (51) have also reported a 2-fold increase in activity after removal of the *N*-glycosylation site at position 384 in LCAT. It is noteworthy that, as is the case with EL, the proposed structure for LCAT also places this particular glycosylation site adjacent to the catalytic triad of the enzyme, raising the possibility that the removal of this glycan increases the accessibility of the substrate to the active site of the enzyme (52).

In our case, removal of the *N*-glycosylation site at position 62 of EL markedly improved the binding affinity of the enzyme only for (A-I)rHDL. Deglycosylation of positions 118 and 473 was also accompanied by significant increases in binding affinity for all four rHDL substrates, the only exception being the interaction of EL N473A with (E4)rHDL, which experienced a substantial loss in binding affinity. Enhanced binding affinity associated with deglycosylation has also been observed for thyrotropin (53) and an anti-CD33 monoclonal antibody (54).

Defective enzyme glycosylation is gaining importance as a diagnostic marker for disease. The results described here raise the possibility that naturally occurring mutations of the *N*-glycosylation sites of EL may significantly affect its activity as well as HDL metabolism. As *N*-glycosylation is a key determinant of both EL activity and substrate specificity, it is an important factor to be taken into consideration when investigating EL-mediated HDL remodeling and its role in atherosclerosis.

The authors thank Kim Tran, Francesca Charlton, and Ewa Kapera for technical assistance and Alison Heather and Jeffrey Cohn for helpful discussions. This research was supported by National Health and Medical Research Council of Australia Grant 222722 and by a Pfizer International HDL Research Award.

REFERENCES

1. Jaye, M., K. J. Lynch, J. Krawiec, D. Marchadier, C. Maugeais, K. Doan, V. South, D. Amin, M. Perrone, and D. J. Rader. 1999. A novel endothelial-derived lipase that modulates HDL metabolism. *Nat. Genet.* **21:** 424–428.
2. Hirata, K., H. L. Dichek, J. A. Cioffi, S. Y. Choi, N. J. Leeper, L. Quintana, G. S. Kronmal, A. D. Cooper, and T. Quertermous. 1999. Cloning of a unique lipase from endothelial cells extends the lipase gene family. *J. Biol. Chem.* **274:** 14170–14175.
3. Ishida, T., S. Choi, R. K. Kundu, K. Hirata, E. M. Rubin, A. D. Cooper, and T. Quertermous. 2003. Endothelial lipase is a major determinant of HDL level. *J. Clin. Invest.* **111:** 347–355.
4. Ma, K., M. Cilingiroglu, J. D. Otvos, C. M. Ballantyne, A. J. Marian, and L. Chan. 2003. Endothelial lipase is a major genetic determinant for high-density lipoprotein concentration, structure, and metabolism. *Proc. Natl. Acad. Sci. USA.* **100:** 2748–2753.
5. Broedl, U. C., W. Jin, and D. J. Rader. 2004. Endothelial lipase: a modulator of lipoprotein metabolism upregulated by inflammation. *Trends Cardiovasc. Med.* **14:** 202–206.
6. McCoy, M. G., G. S. Sun, D. Marchadier, C. Maugeais, J. M. Glick, and D. J. Rader. 2002. Characterization of the lipolytic activity of endothelial lipase. *J. Lipid Res.* **43:** 921–929.
7. Kobayashi, Y., T. Nakajima, and I. Inoue. 2002. Molecular modeling of the dimeric structure of human lipoprotein lipase and functional studies of the carboxyl-terminal domain. *Eur. J. Biochem.* **269:** 4701–4710.
8. van Tilbeurgh, H., A. Roussel, J. M. Lalouel, and C. Cambillau. 1994. Lipoprotein lipase. Molecular model based on the pancreatic lipase X-ray structure: consequences for heparin binding and catalysis. *J. Biol. Chem.* **269:** 4626–4633.
9. Perret, B., L. Mabile, L. Martinez, F. Terce, R. Barbaras, and X. Collet. 2002. Hepatic lipase: structure/function relationship, synthesis, and regulation. *J. Lipid Res.* **43:** 1163–1169.
10. Winkler, F. K., A. D'Arcy, and W. Hunziker. 1990. Structure of human pancreatic lipase. *Nature.* **343:** 771–774.
11. van Tilbeurgh, H., L. Sarda, R. Verger, and C. Cambillau. 1992. Structure of the pancreatic lipase-procolipase complex. *Nature.* **359:** 159–162.
12. Miller, G. C., C. J. Long, E. D. Bojilova, D. Marchadier, K. O. Badellino, N. Blanchard, I. V. Fuki, J. M. Glick, and D. J. Rader. 2004. Role of N-linked glycosylation in the secretion and activity of endothelial lipase. *J. Lipid Res.* **45:** 2080–2087.
13. Shimokawa, Y., K. Hirata, T. Ishida, Y. Kojima, N. Inoue, T.

Quertermous, and M. Yokoyama. 2005. Increased expression of endothelial lipase in rat models of hypertension. *Cardiovasc. Res.* **66:** 594–600.
14. Jin, W., J. S. Millar, U. Broedl, J. M. Glick, and D. J. Rader. 2003. Inhibition of endothelial lipase causes increased HDL cholesterol levels in vivo. *J. Clin. Invest.* **111:** 357–362.
15. Lis, H., and N. Sharon. 1993. Protein glycosylation. Structural and functional aspects. *Eur. J. Biochem.* **218:** 1–27.
16. Helenius, A., and M. Aebi. 2001. Intracellular functions of N-linked glycans. *Science.* **291:** 2364–2369.
17. Dwek, R. A. 1996. Glycobiology: toward understanding the function of sugars. *Chem. Rev.* **96:** 683–720.
18. Wicker-Planquart, C., S. Canaan, M. Riviere, and L. Dupuis. 1999. Site-directed removal of N-glycosylation sites in human gastric lipase. *Eur. J. Biochem.* **262:** 644–651.
19. Vinals, M., S. Xu, E. Vasile, and M. Krieger. 2003. Identification of the N-linked glycosylation sites on the high density lipoprotein (HDL) receptor SR-BI and assessment of their effects on HDL binding and selective lipid uptake. *J. Biol. Chem.* **278:** 5325–5332.
20. Gavel, Y., and G. von Heijne. 1990. Sequence differences between glycosylated and non-glycosylated Asn-X-Thr/Ser acceptor sites: implications for protein engineering. *Protein Eng.* **3:** 433–442.
21. Weisgraber, K. H. 1994. Apolipoprotein E: structure-function relationships. *Adv. Protein Chem.* **45:** 249–302.
22. Krimbou, L., M. Tremblay, J. Davignon, and J. S. Cohn. 1997. Characterization of human plasma apolipoprotein E-containing lipoproteins in the high density lipoprotein size range: focus on pre-beta1-LpE, pre-beta2-LpE, and alpha-LpE. *J. Lipid Res.* **38:** 35–48.
23. Zhang, B., P. Fan, E. Shimoji, H. Xu, K. Takeuchi, C. Bian, and K. Saku. 2004. Inhibition of cholesteryl ester transfer protein activity by JTT-705 increases apolipoprotein E-containing high-density lipoprotein and favorably affects the function and enzyme composition of high-density lipoprotein in rabbits. *Arterioscler. Thromb. Vasc. Biol.* **24:** 1910–1915.
24. Caiazza, D., A. Jahangiri, D. J. Rader, D. Marchadier, and K. A. Rye. 2004. Apolipoproteins regulate the kinetics of endothelial lipase-mediated hydrolysis of phospholipids in reconstituted high-density lipoproteins. *Biochemistry.* **43:** 11898–11905.
25. Rye, K. A., K. H. Garrety, and P. J. Barter. 1992. Changes in the size of reconstituted high density lipoproteins during incubation with cholesteryl ester transfer protein: the role of apolipoproteins. *J. Lipid Res.* **33:** 215–224.
26. Lund-Katz, S., M. Zaiou, S. Wehrli, P. Dhanasekaran, F. Baldwin, K. H. Weisgraber, and M. C. Phillips. 2000. Effects of lipid interaction on the lysine microenvironments in apolipoprotein E. *J. Biol. Chem.* **275:** 34459–34464.
27. Hime, N. J., K. J. Drew, C. Hahn, P. J. Barter, and K. A. Rye. 2004. Apolipoprotein E enhances hepatic lipase-mediated hydrolysis of reconstituted high-density lipoprotein phospholipid and triacylglycerol in an isoform-dependent manner. *Biochemistry.* **43:** 12306–12314.
28. Rye, K. A., N. J. Hime, and P. J. Barter. 1996. The influence of sphingomyelin on the structure and function of reconstituted high density lipoproteins. *J. Biol. Chem.* **271:** 4243–4250.
29. Piran, U., and R. J. Morin. 1979. A rapid radioassay procedure for plasma lecithin-cholesterol acyltransferase. *J. Lipid Res.* **20:** 1040–1043.
30. Matz, C. E., and A. Jonas. 1982. Micellar complexes of human apolipoprotein A-I with phosphatidylcholines and cholesterol prepared from cholate-lipid dispersions. *J. Biol. Chem.* **257:** 4535–4540.
31. Rye, K. A., and P. J. Barter. 1994. The influence of apolipoproteins on the structure and function of spheroidal, reconstituted high density lipoproteins. *J. Biol. Chem.* **269:** 10298–10303.
32. Thuren, T., K. H. Weisgraber, P. Sisson, and M. Waite. 1992. Role of apolipoprotein E in hepatic lipase catalyzed hydrolysis of phospholipid in high-density lipoproteins. *Biochemistry.* **31:** 2332–2338.
33. Chiba, H., M. Eto, S. Fujisawa, K. Akizawa, S. Intoh, O. Miyata, K. Noda, K. Matsuno, and K. Kobayashi. 1993. Increased plasma apolipoprotein E-rich high-density lipoprotein and its effect on serum high-density lipoprotein cholesterol determination in patients with familial hyperalphalipoproteinemia due to cholesteryl ester transfer activity deficiency. *Biochem. Med. Metab. Biol.* **49:** 79–89.
34. Johnson, M. M., and J. P. Peters. 1993. Technical note. An improved method to quantify nonesterified fatty acids in bovine plasma. *J. Anim. Sci.* **71:** 753–756.
35. Takayama, M., S. Itoh, T. Nagasaki, and I. Tanimizu. 1977. A new enzymatic method for determination of serum choline-containing phospholipids. *Clin. Chim. Acta.* **79:** 93–98.
36. Stahler, F., W. Gruber, K. Stinshoff, and P. Roschlau. 1977. A practical enzymatic cholesterol determination. *Med. Lab. (Stuttg.).* **30:** 29–37.
37. Smith, P. K., R. I. Krohn, G. T. Hermanson, A. K. Mallia, F. H. Gartner, M. D. Provenzano, E. K. Fujimoto, N. M. Goeke, B. J. Olson, and D. C. Klenk. 1985. Measurement of protein using bicinchoninic acid. *Anal. Biochem.* **150:** 76–85.
38. Rainwater, D. L., D. W. Andres, A. L. Ford, F. Lowe, P. J. Blanche, and R. M. Krauss. 1992. Production of polyacrylamide gradient gels for the electrophoretic resolution of lipoproteins. *J. Lipid Res.* **33:** 1876–1881.
39. Badellino, K. O., M. L. Wolfe, M. P. Reilly, and D. J. Rader. 2006. Endothelial lipase concentrations are increased in metabolic syndrome and associated with coronary atherosclerosis. *PLoS Med.* **3:** 245–252.
40. Semenkovich, C. F., C. C. Luo, M. K. Nakanishi, S. H. Chen, L. C. Smith, and L. Chan. 1990. In vitro expression and site-specific mutagenesis of the cloned human lipoprotein lipase gene. Potential N-linked glycosylation site asparagine 43 is important for both enzyme activity and secretion. *J. Biol. Chem.* **265:** 5429–5433.
41. Busca, R., M. A. Pujana, P. Pognonec, J. Auwerx, S. S. Deeb, M. Reina, and S. Vilaro. 1995. Absence of N-glycosylation at asparagine 43 in human lipoprotein lipase induces its accumulation in the rough endoplasmic reticulum and alters this cellular compartment. *J. Lipid Res.* **36:** 939–951.
42. Wolle, J., H. Jansen, L. C. Smith, and L. Chan. 1993. Functional role of N-linked glycosylation in human hepatic lipase: asparagine-56 is important for both enzyme activity and secretion. *J. Lipid Res.* **34:** 2169–2176.
43. Ben-Zeev, O., G. Stahnke, G. Liu, R. C. Davis, and M. H. Doolittle. 1994. Lipoprotein lipase and hepatic lipase: the role of asparagine-linked glycosylation in the expression of a functional enzyme. *J. Lipid Res.* **35:** 1511–1523.
44. Brown, R. J., G. C. Miller, N. Griffon, C. J. Long, and D. J. Rader. 2007. Glycosylation of endothelial lipase at asparagine-116 reduces activity and the hydrolysis of native lipoproteins in vitro and in vivo. *J. Lipid Res.* **48:** 1132–1139.
45. Broedl, U. C., W. Jin, I. V. Fuki, J. M. Glick, and D. J. Rader. 2004. Structural basis of endothelial lipase tropism for HDL. *FASEB J.* **18:** 1891–1893.
46. Saito, H., S. Lund-Katz, and M. C. Phillips. 2004. Contributions of domain structure and lipid interaction to the functionality of exchangeable human apolipoproteins. *Prog. Lipid Res.* **43:** 350–380.
47. Razzaghi, H., B. W. Day, R. J. McClure, and M. I. Kamboh. 2001. Structure-function analysis of D9N and N291S mutations in human lipoprotein lipase using molecular modelling. *J. Mol. Graph. Model.* **19:** 487–494, 587–590.
48. Helenius, A., and M. Aebi. 2004. Roles of N-linked glycans in the endoplasmic reticulum. *Annu. Rev. Biochem.* **73:** 1019–1049.
49. Stahnke, G., R. C. Davis, M. H. Doolittle, H. Wong, M. C. Schotz, and H. Will. 1991. Effect of N-linked glycosylation on hepatic lipase activity. *J. Lipid Res.* **32:** 477–484.
50. Gotte, G., M. Libonati, and D. V. Laurents. 2003. Glycosylation and specific deamidation of ribonuclease B affect the formation of three-dimensional domain-swapped oligomers. *J. Biol. Chem.* **278:** 46241–46251.
51. O, K., J. S. Hill, X. Wang, R. McLeod, and P. H. Pritchard. 1993. Lecithin:cholesterol acyltransferase: role of N-linked glycosylation in enzyme function. *Biochem. J.* **294:** 879–884.
52. Peelman, F., N. Vinaimont, A. Verhee, B. Vanloo, J. L. Verschelde, C. Labeur, S. Seguret-Mace, N. Duverger, G. Hutchinson, J. Vandekerckhove, et al. 1998. A proposed architecture for lecithin cholesterol acyl transferase (LCAT): identification of the catalytic triad and molecular modeling. *Protein Sci.* **7:** 587–599.
53. Berman, M. I., C. G. Thomas, Jr., P. Manjunath, M. R. Sairam, and S. N. Nayfeh. 1985. The role of the carbohydrate moiety in thyrotropin action. *Biochem. Biophys. Res. Commun.* **133:** 680–687.
54. Co, M. S., D. A. Scheinberg, N. M. Avdalovic, K. McGraw, M. Vasquez, P. C. Caron, and C. Queen. 1993. Genetically engineered deglycosylation of the variable domain increases the affinity of an anti-CD33 monoclonal antibody. *Mol. Immunol.* **30:** 1361–1367.